

# The Morphology of SiO<sub>x</sub> Coated PET Coating by Ultrasonic Atomic Force Microscopy and Barrier Properties

Zhang Gaimei<sup>1, 2, a</sup>, Chen Qiang<sup>1</sup>, He Cunfu<sup>2</sup>, Zhang Shouye<sup>1</sup>

<sup>1</sup>Beijing Institute of Graphic Communication, Beijing 102600, China

<sup>2</sup>College of Mechanical Engineering & Applied Electronics Technology, Beijing University of Technology, Beijing 100124, China

aemail: zhang\_gaimei@163.com

**Keywords:** SiO<sub>x</sub> coating, plastic barrier properties, UAFM, subsurface defect, ultrasonic amplitude image

**Abstract:** The oxygen transmission rate (OTR) of SiO<sub>x</sub> coated polyethylene terephthalate (PET) and biaxially oriented polypropylene (BOPP) affected by fine defects is discussed in this paper. With an ultrasonic AFM (UAFM), which is an advantageous to distinguishing tiny defects on/ in the deposited films, it is found that the OTR of the coated films is relevant to the morphology scanned by UAFM. Herein SiO<sub>x</sub> layers with a thickness in the order of nano-scale were fabricated in 13.56 MHz-radio frequency (RF) -plasma-enhanced chemical vapor deposition (PECVD). The monomer for the coating fabrication is hexamethyldisiloxane (HMDSO). Fourier transform infrared (FTIR) spectra of the deposited coating with a strong peak at 1062 cm<sup>-1</sup>, corresponding to Si-O-Si stretching vibration, confirm the formation of SiO<sub>x</sub> coatings through PECVD. The higher OTR value of SiO<sub>x</sub> coated PET is consistent with defects on film surface and in the subsurface of coatings through UAFM. It obtains that the OTR value of the defect free SiO<sub>x</sub> coated film was reduced by ca. 89% compared with the defect existence SiO<sub>x</sub> coated PET.

## Introduction

Plasma enhanced chemical vapor deposition (PECVD) has been often utilized to deposit SiO<sub>x</sub> films on plastic substrates<sup>[1]</sup> to improve their gas-barrier properties, and its applications have got more and more attention in industries of pharmacy<sup>[2]</sup>, food and beverage packaging<sup>[3]</sup> due to excellent gas-barrier properties but keeping with a visible-light transparency. But in fact the oxygen transmission rate (OTR) of “soft-glass” SiO<sub>x</sub> coated PET is still much higher than that of solid-state glasses. One of the possible reasons is attributed to defects both on the surface of and in the subsurface formed during SiO<sub>x</sub> coating deposition. The detection of these nano-scale tiny defects is very difficult by conventional methods<sup>[4]</sup>. In order to well understand the mechanism of SiO<sub>x</sub> coated PET films still have high OTR value, the detection method should be improved and innovated. An ultrasonic atomic force microscopy (UAFM) demonstrates an advantageous in the detection of tiny defects comparing with a conventional atomic force microscopy (AFM) and scanning electron microscopy (SEM)<sup>[5-7]</sup>. Even a cross-sectional high-resolution transmission electron microscopy (HRTEM) can be utilized to detect defects in coatings, the complex process and the frequent damages of sample preparation prior to the investigation of morphology make HRTEM measurement being low efficiency and waste time work<sup>[8-10]</sup>.

Based on the scanning of surface morphology and OTR value measurement of SiO<sub>x</sub> coated PET films, we obtain that the UAFM method proposed in the present paper is effective to detect tiny defects. The improvement of our UAFM system is that the cantilever with a sensor tip is vibrated forcedly by an ultrasonic waveform. Due to ultrasonic waveform vibration, the images obtained from UAFM shall depend on elastic modulus of the coatings, therefore, the different elastic modulus caused from defects can be distinguished easily from the AFM images. Consistence with the measurement of OTR value of SiO<sub>x</sub> coated PET, it is clear that minimum OTR value of 0.539 cc/m<sup>2</sup>/day of SiO<sub>x</sub> coated PET was due to defect-free in the surface and subsurface, which is ca. 10 times smaller than that defect existence SiO<sub>x</sub> coated PET films.

## Experiment

### 2.1 SiO<sub>x</sub> deposition

The processes of SiO<sub>x</sub> coating were as followings; substrates polyethylene terephthalate (PET) and biaxially-oriented polypropylene (BOPP) films were cleaned ultrasonically in the ethanol, acetone and de-ionized water for 5 min in consequent before mounted on a sample holder. Figure 1 shows a photo (a) and schematic diagram (b) of experimental facilities. SiO<sub>x</sub> coatings were deposited in a radio frequency (RF, 13.56 MHz)-PECVD. During the process, the flow rates of oxygen and monomer hexamethyldisiloxane (HMDSO) were fixed at 20 sccm and at 10 sccm, respectively. The RF power was kept at 200W, except the deposition time was varied from 10, 20 to 30 minutes.

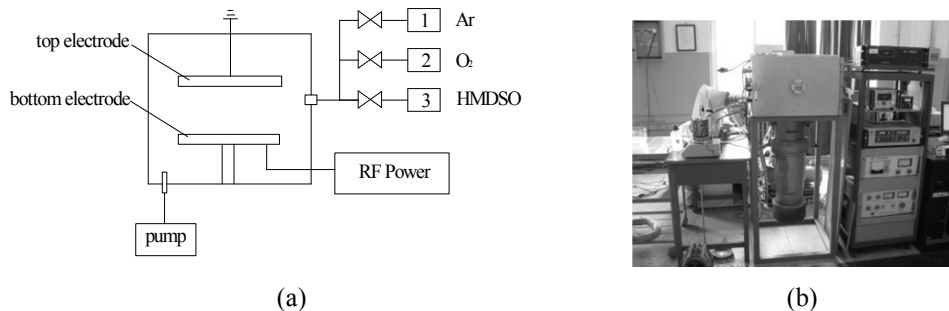


Fig.1 The schematic diagram of the plasma setup (a) and photo of plasma setup(b)

### 2.2 Analysis of the chemical structure and measurement of OTR

The chemical structure of SiO<sub>x</sub>-coatings were characterized by Fourier transform infrared spectroscopy (FTIR) (Shimadzu, FTIR-8400, Japan). The property of SiO<sub>x</sub> coated films were carried out in oxygen permeation analyzer (Illinois Instruments, model 8001, USA) for OTR measurement, where the humidity is kept at 0 or 65% at a room temperature of 23 °C.

### 2.3 UAFM analysis

Figure 2 shows a schematic diagram of the UAFM system, where a sample was vibrated by ultrasonic waveform at the frequencies 100 kHz and 250 kHz. The tip-sample was contacted by setting the contact mode in AFM measurement. The displacement of cantilever vibration induced by ultrasonic waveform was monitored by photo-diode detector. Then the images obtained from original contact-mode AFM and ultrasonic amplitudes were simultaneously recorded at the same region of sample [11-12]. The images, depending on the elastic modulus and stiffness of scanned samples, were used to evaluate defect status in samples based on this resonance frequency shifting [13-17].

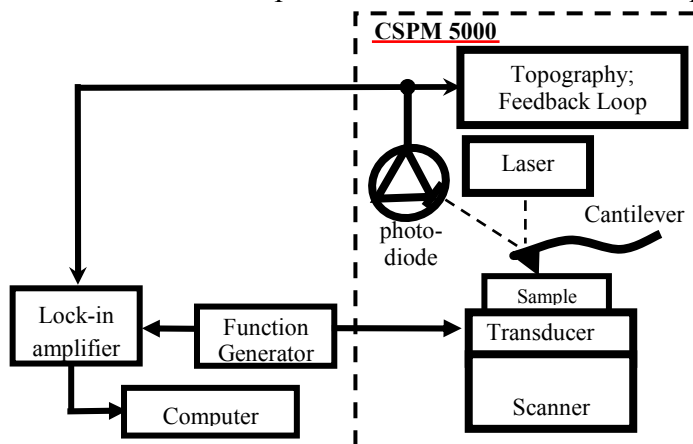


Fig.2 Block diagram of UAFM system

### 2.4 Thickness measurement

Thickness of deposited SiO<sub>x</sub> coatings was measured by surface profiler (Veeco, Dektak 150, USA). The deposition rate can be obtained based on the variation of the exposure times.

## Results and discussion

### 3.1 FTIR spectra and deposition rate

Figure 3 shows FTIR spectra of as-prepared films at the exposure times of 10, 20, and 30 min, respectively, where the working pressure is 20 Pa and an applied power is 200 W. The SiO<sub>x</sub> formation is confirmed from the FTIR spectra. It is seen that the film components did not change through the exposure time. The absorption peaks at 805 cm<sup>-1</sup> and 1062 cm<sup>-1</sup> assumed to the bending and stretching vibration of Si-O-Si bond<sup>[8]</sup> respectively are obviously appeared in the spectra. In particular the absorption peaks in the range of 1030 to 1070 cm<sup>-1</sup> for stretching vibrations of Si-O-Si are significantly increased along with the exposure time. So did the peak at the range of 795–810 cm<sup>-1</sup> for Si-O-Si vibrations.

Figure 4 shows the deposition rate of SiO<sub>x</sub> coatings as a function of the exposure time. It is seen that the deposition rate is 9 nm/min at exposure time of 10 min, but decreasing to 5.5 nm/min at 20 min. The deposition rate interestingly increased to 8.3 nm/min when exposure time was extended to 30 min.

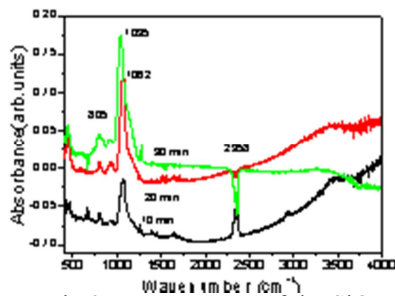


Fig.3 FTIR spectra of the SiO<sub>x</sub> coatings in different discharge times

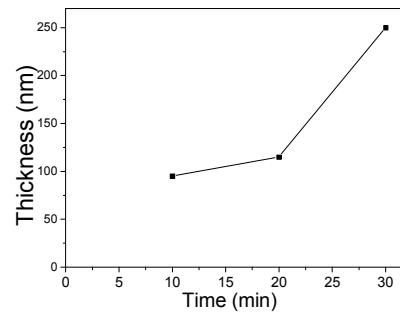


Fig.4 The film thickness versus the discharge time

### 3.2 UAFM and AFM images

It is known that AFM images demonstrate in dark regions with a black color, and in bright regions with a white color, which depend on the low/high depth in morphology in contact mode. With the ultrasonic waveform applied to the samples the ultrasonic amplitude images based on the magnified cantilever amplitude should provide the valuable images, where the brightness is relevant to the cantilever amplitude. The higher amplitude, the whiter of the brightness in the images.

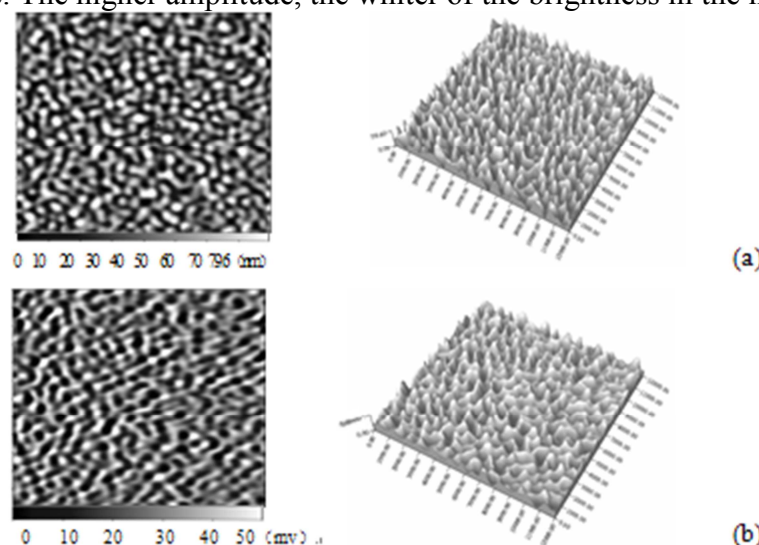


Fig.5 Topography (a) and the ultrasonic amplitude image (b) for SiO<sub>x</sub> coatings excited at the 100 kHz (deposition conditions: 200W, 20Pa, 20 min and the ratio of O<sub>2</sub>/HMDSO = 2:1, in the continuous mode)

Based on the Hertz contact theory<sup>[13]</sup> and the vibration modulus<sup>[13]</sup> of the AFM micro-cantilever, the image contrast obtained from the ultrasonic amplitude depends on the average resonance frequency and ultrasonic frequency. Therefore, the image contrast varies with the ultrasonic frequency (hereafter, this is called excitation frequency).

Fig. 5 (a) and (b) are a typical topography image (unit in nm) and an ultrasonic amplitude image (unit in mV) of SiO<sub>x</sub> coatings excited at a frequency of 100 kHz, respectively. One can see that the brightness in two images are inversed in the whole area, which means in these cases the defects are absence from the surface/subsurface on as-deposited coatings.

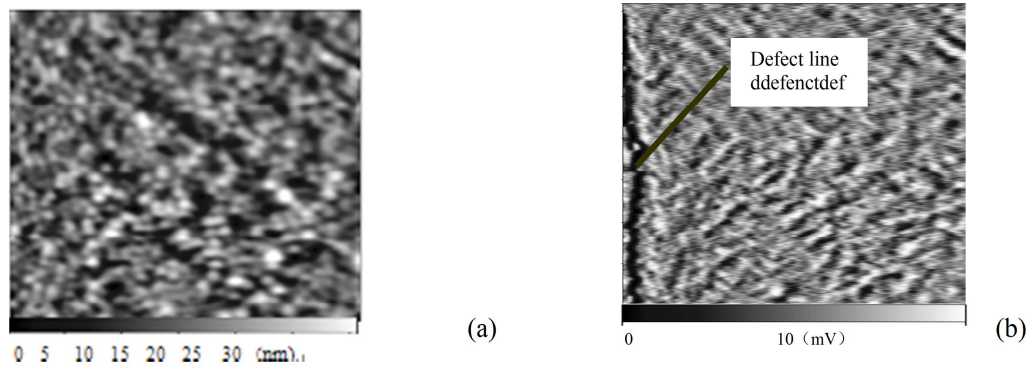


Fig.6 Topography (a), and ultrasonic amplitude (b) images of deposited SiO<sub>x</sub> coating excited at frequency of 250 kHz.

The topography and ultrasonic amplitude images in Fig. 6 (a) and (b) were obtained at an excitation frequency of 250 kHz. One can see that color contrast and brightness in both images is identical in near all area except a black line in (b), an inversed color brightness area, which indicates the existence of line defects on the subsurface. It means by comparing the image obtained from UAFM and topography, the defects can be distinguished simply from images.

The reason is that the topography image can only reveal the morphology of the as-prepared coating, and the information under the subsurface can not be scanned based on this method. With an ultrasonic waveform applied on the substrate, however, the different elastic modulus and the local contact stiffness between the tip of probe and sample shall lead to a variation of resonance frequency and amplitude of cantilever, which can reveal the surface and subsurface structures qualitatively in ultrasonic amplitude image.

### 3.3. Barrier property

Table 1 shows OTR values of control PET and BOPP, and SiO<sub>x</sub> coated ones in humidities of 0% and 65%, respectively. One can see that the OTR values were significantly reduced comparing to the control samples. For 70 μm-thick PET samples, OTR values of SiO<sub>x</sub> coated ones reduce from 21.4 cc/m<sup>2</sup>/day and 17.3 cc/m<sup>2</sup>/day to 5.71 cc/m<sup>2</sup>/day and 4.77 cc/m<sup>2</sup>/day at humidities of 0 and 65%, respectively; For BOPP, these value were reduced from 2031 cc/m<sup>2</sup>/day and 1853 cc/m<sup>2</sup>/day to 42.1 cc/m<sup>2</sup>/day and 37.8 cc/m<sup>2</sup>/day, respectively.

Films	Thickness (μm)	OTR (cc/m <sup>2</sup> /day) (23±0.5°C)	
		Humidity0%	Humidity65%
Original PET	70	21.4	17.3
SiO <sub>x</sub> coated PET	70±0.090	5.71	4.77
Original BOPP	18	2031	1853
SiO <sub>x</sub> coated BOPP	18±0.090	42.1	37.8

Comparing to the minimum OTR value of 0.539 cc/m<sup>2</sup>/day obtained from SiO<sub>x</sub> coated PET (12.5 μm in thickness) in our experiment, or 100 nm-thick aluminum foil coated PET 0.5 cc/m<sup>2</sup>/day (25 μm in thickness, a relative humidity of 30%)<sup>[18]</sup>, the OTR value in table.1 is rather high. Based on the Fig. 5 and Fig. 6 thus, it can presume that OTR value is dominated by defects in surface and subsurface. Therefore the quality of the SiO<sub>x</sub> coatings can be improved by the detection of the subsurface defects in sample with ultrasonic amplitude images based on UAFM system.

### 3.4 Discussion

In UAFM system, an ultrasonic waveform is generated by a piezoelectric transducer after applying an AC power, which gives a stress to the sample. The amplitude of the cantilever reflects the locally-generated contact stiffness between the tip of the cantilever and the sample. Besides, the contact stiffness is closely relevant to the elastic stress in the sample.

In figure 7 the spectra of the vibration frequency indicates the contact stiffness in two cases: the excitation frequency 1 (noted as  $f_1$ ) at line (1) is smaller than that the frequency (noted as  $f_0$ ) at cross point of the two contact stiffness  $k^*$ ; The excitation frequency 2 (noted as  $f_2$ ) at line (2) is larger than  $f_0$ . One can see that a bright image or a high amplitude of ultrasonic amplitude image assumed to the small stiffness [5] can be obtained when the excitation frequency is smaller than  $f_0$ . Whereas when the excitation frequency is larger than  $f_0$  the soft areas (corresponding to small stiffness) shows a dark image.

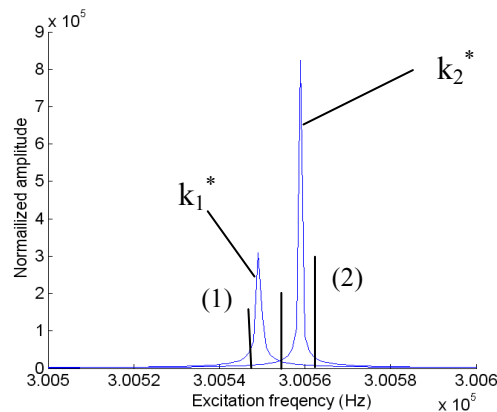


Fig. 7 The frequency spectroscopy of the cantilever at the different contact stiffness  $k^*$

When the tip scans a high region in the topography image, the repulsion between tip and sample is larger. Equivalently the contact stiffness in the high region is larger than that in the low region. If the excitation frequency is near the contact response frequency, the ultrasonic amplitude of the cantilever is higher than that in the stiff regions, thus the brightness is inverse in these two images as shown in Fig. 5 (a) and (b). However, when the excitation frequency is near the stiff regions (high region in topography image), the ultrasonic amplitude of the cantilever is higher, therefore the brightness is identical in the two images as shown Fig. 6 (a) and 6(b) [17].

It is well known that in the subsurface defect areas, the contact stiffness of tip-to-sample is small, i.e. the resonance frequency is smaller than the centre vibration frequency. The excitation frequency shall be far away from the resonance frequency, which leads to the cantilever amplitude being small as showed in Fig. 6 (b).

### Conclusions

In this paper, a novel method UAFM for defects in surface and subsurface of as-deposited SiOx was proposed. SiOx coatings were prepared by RF (13.56 MHz)-PECVD and deposited on PET film. Based on AFM and UAFM images the significant enhancement of the gas barrier property of coated PET was explained by the compact structure of SiOx coatings. It results that UAFM is an efficient method in nondestructive measurement. The relatively high OTR value of SiOx coating PET can be reasonably explained through the UAFM image, where defects in surface and in subsurface can be clearly detected in UAFM image. It concludes that gas barrier property can be improved by avoiding defect in surface and in subsurface of the as-deposited coatings.

## Acknowledgement

This work was supported by the national natural science foundation (No.50775005), the Distinguish Scholar Foundation of Organization Department, Beijing Government (No.09000001) and General program of science and technology development project of Beijing Municipal Education Commission(No.KM201110015009).

## References

- [1] Zhou Mei-Li, Fu Ya-Bo, Chen qiang Ge Yuanjing Chinese Phys. 16(2007) 1101
- [2] X. Zhu, F.A. Khonsari, C.P. Etienne, M. Tatoulian, Plasma Process. Polym. 2 (2005) 407.
- [3] Dennler G, Houdayer A, Segui Y, Wertheimer M R, J. Vac. Sci. Technol. A 19 (2001) 2320
- [4]A. Gruniger, Ph. Rudolf von Rohr, Thin Solid Films 459(2004) 308
- [5] Garcia-Ayuso, G.; Vazquez, L.; Martinez-Duart,Surf. Coat. Technol. 80 (1996) 203
- [6] Barker, C. P.; Kochem, K. H.; Revell, K. M.,Thin Solid Films 259 (1995) 46
- [7] R. R. Mallik, T. Butler, Jr., W. J. Kulnis, Jr., T. S. Confer, and P. N. Henriksen, Journal of Vacuum Science & Technology A: Vacuum, Surfaces, and Films 10(1992) 2412
- [8] R. Thyen., A. Weber, C. P. Klages, Surf. Coat. Technol. 97(1997) 426
- [9] Philips, R. W.; Markantes, T.; LeGallee, C. SVC 36th Annu. Technol. Conf. Proc. 1993, 293
- [10] Henry, B. M.; Roberts, A. P.; Grovenor, C. R. M.; Sutton, A. P.; Briggs, G. A. D.; Tsukahara, Y.; Miyamoto, Y. M.; Chater, R. J. SVC 41st Annu. Technol. Conf. Proc. 1998, 434
- [11] M.Teresa Cubers, Journal of Physics Conference Series .100(2008) 052013
- [12] J.T. ZENG, K.Y. ZHAO, H.R.ZENG, H.Z.SONG, L.Y.ZHENG, G.R.LI, Q.R.YIN Appl.Phys. A. 91(2008) 261
- [13] He cunfu, Zhang Gaimei, Wu Bin, Wu Zaiqi, Optics and Lasers in Engineering. 48(1010) 1108
- [14] D. Passeri, M. Rossi, A.Alippi, A.Bettucci, M.L.Terranova, E. Tamburri, F. Toschi, Physica E. 40 (2007) 2419
- [15] U. Rabe, S. Amelio, E. Kester, V. Scherer, S. Hirsekorn, W. Arnold, Ultrasonics. 38(2003) 430
- [16] D C Hurley, K. Shen, N.M. Jennett, J.A. Turner, J. Appl. Phys. 94(2003) 2347
- [17] U. Rabe, S. Amelio, M. Kopycinska, S. Hirsekorn, M. Kempf, M. Göken , W. Arnold, Surf. Interface Anal. 33(2002) 65.
- [18] U. Moosheimer, Ch. Bichler, Surf. Coat. Technol. 116-119 (1999) 812